Separation and Purification Technology 73 (2010) 8–12

Contents lists available at ScienceDirect

Separation and Purification Technology

journal homepage: www.elsevier.com/locate/seppur

Microporous titanosilicate ETS-10 membrane for high pressure CO_2 separation

Inés Tiscornia [a], Izumi Kumakiri [b], Rune Bredesen [b], Carlos Téllez [a,*], Joaquín Coronas [a]

[a] Department of Chemical and Environmental Engineering, Nanoscience Institute of Aragon, Universidad de Zaragoza, 50018 Zaragoza, Spain
[b] SINTEF Materials and Chemistry, P-B- 124 Blindern, 0314 Oslo, Norway

ARTICLE INFO

Keywords:
Microporous titanosilicate
ETS-10
Zeolite membrane
CO_2 separation
High pressure

ABSTRACT

Membrane technology is expected to be an efficient process for CO_2 separation. Microporous titanosilicate ETS-10 membranes prepared by seeded hydrothermal synthesis are presented as candidates to CO_2 separation from binary mixtures (CO_2/N_2 and CO_2/H_2). The prepared membranes with different synthesis time have been characterized by SEM and XRD. Permeation properties have been evaluated by a novel, non-destructive technique based on the measurement of the local He permeation of a limited area. It was established a good concordance between defects localized by the new He mapping technique and the separation properties of the membranes. At room temperature, ETS-10 membranes can separate CO_2/N_2 equimolar mixture with separation factors between 7–10 in the 6–22 bar pressure range.

1. Introduction

The use of fossil fuels as energetic vector leads to CO_2 emissions into the atmosphere, which may contribute to global warming. Independently of how CO_2 capture is integrated in power generation processes employing fossil combustibles (e.g. in post-combustion, oxy-fuel combustion, pre-combustion decarbonisation cycles), it is low efficiency and cost penalty. Furthermore, in natural gas sweetening, CO_2 is removed because it causes pipeline corrosion, reduces the heating value and increases transport cost. The replacement of the more-common separation operations (chemical absorption and physical adsorption) by membrane separation could save energy and cost in the CO_2 capture process [1]. Membrane materials including polymers [2–4] and inorganic molecular sieves [5–7] with high selectivity for CO_2 over O_2, N_2 or CH_4 have been developed.

Zeolite membranes are microporous inorganic membranes that have been reported in a wide variety of applications such as in separation of isomers [8], gas mixtures [9] and pervaporation [10]. Their seemingly high thermal, mechanical and chemical stability, and the adsorption capacity of zeolitic pores of molecular dimension with specific permeating compounds enable this broad use. In the case of e.g. CO_2/N_2, CO_2/CH_4, and CO_2/H_2 mixtures, CO_2 adsorbs more strongly and permeate preferentially through the membrane. For the CO_2/N_2 and CO_2/CH_4 mixtures, CO_2 is smaller in size and thus permeates faster also at elevated temperature but the selectivities are very low due to the absence of effective adsorption. FAU-type zeolite membranes have been used to separate CO_2 from N_2 [5,11,12], achieving a CO_2/N_2 separation factor of 100 at 303 K [11]. Permeation properties of the ion-exchanged FAU-type zeolite membranes for single-component and binary mixture systems of CO_2 and N_2 have also been investigated [13].

MFI-type membranes have shown considerably lower CO_2/N_2 separation factors [14–16]. Recently, the properties of MFI-type zeolite membranes (ion exchange Na-ZSM-5 and boron-substituted ZSM-5 membranes) working at high pressure (up to 30 bar) have been studied [17]. The best results from this work were obtained with a boron-substituted ZSM-5 membrane prepared over a tubular porous stainless steel support: a combined CO_2 permeance of 2.66×10^{-7} mol/m^2 s Pa and CO_2/N_2 separation factor of 13. ZSM-5 zeolite membranes were also surface-modified by dip-coating with polymeric silica sol which filled up the intercrystalline voids in order to improve the CO_2 separation efficiency [18]. Membranes made of pseudozeolites such as SAPO-34 (a chabazite analog) have shown a promising performance in this system [19–21].

The synthesis and application of microporous titanosilicates, related materials possessing framework structures and mixed octahedral–pentahedral–tetrahedral microporous (OPT) siliceous frameworks have been extensively studied since the discovery of ETS-10 and ETS-4 in late 1980s [22,23]. As typical zeolites, these materials can act as heterogeneous catalysts in a number of important chemical processes, where the strong basic character combined with the spatial constraints plays an important role [24,25]. Also, due to the adsorption [26] and ion exchange [27] properties, ETS-10 membranes have been used for the dehydration by pervaporation of water/alcohol [28,29] and water/acid acetic [29] mixtures, and for the gas phase separation of propylene/propane mixtures [30,31].

* Corresponding author at: Chemical and Environmental Engineering Department, Universidad de Zaragoza, Centro Politécnico Superior, c/ María de Luna, 3, 50018 Zaragoza, Spain. Tel.: +34 976 762471; fax: +34 976 761879.
E-mail address: ctellez@unizar.es (C. Téllez).

1383-5866/$ – see front matter © 2009 Elsevier B.V. All rights reserved.
doi:10.1016/j.seppur.2009.07.008

Table 1
Characteristics, weight gain (mg of zeolite/g of support), N_2 single gas permeance at ambient temperature, CO_2/N_2 and CO_2/H_2 separation properties at ambient temperature of the ETS-10 membranes tested in this work. Separation: feed: 100 mL(STP)/min of a 50/50 CO_2/N_2 or CO_2/H_2 mixture, Ar sweep gas: 60 mL(STP)/min, permeate at atmospheric pressure and $\Delta P = 0.08$ bar between retentate and permeate.

Membrane	ETS10-8	ETS10-24	ETS10-48
Synthesis time (h)	8	24	48
Weight gain (mg/g)	13	35	68
N_2 permeance $\times 10^8$ (mol/m^2 s Pa) single gas	5.5	1.8	0.25
CO_2/N_2 separation factor in mixture	6.0	10	–[a]
CO_2 permeance $\times 10^8$ (mol/m^2 s Pa) in CO_2/N_2 mixture	4.7	2.8	–[a]
CO_2/H_2 separation factor in mixture	–[a]	9.0	–[a]
C_3H_6/C_3H_8 separation factor in mixture[b]	5.0	4.6	3.2
C_3H_6 permeance $\times 10^8$ (mol/m^2 s Pa) in mixture[b]	4.5	3.9	0.32

[a] Not measured.
[b] From Ref. [31] of a 30/70 propylene/propane mixture at 30 °C and $\Delta P = 100$ 1 bar.

In this work, ETS-10 membranes are synthesized on the external surface of porous alumina tubes by a recently published procedure [31]. The CO_2 separation performance of the membranes is characterized in CO_2/N_2 and CO_2/H_2 mixtures at high pressure (up to 22 bar). Defects in the membranes were localized and visualized by a novel, non-destructive technique recently developed [32]. The technique is based on measuring the local He permeation supplied by a microscopic needle to a limited area of the membrane surface.

2. Experimental

The ETS-10 membranes were prepared on the outside part of symmetric α-alumina supports (Inocermic, 1900 nm pore size) using the method previously described [31]. Before the hydrothermal synthesis, the outside surface of the support was seeded by rubbing with ETS-10 seeds (ETS-10 seeds with a particle size of approximately 500 nm [26]). The internal and external diameters of the tubes were 7 and 10 mm, respectively, with 8 cm length of which 5 cm were permeable (remaining parts were closed by enamelling). The ETS-10 gel had the following molar composition: 10 NaOH:4 KF:1 TiO_2:10 SiO_2:675 H_2O. Hydrofluoric acid (48 wt.% in water, Merck) was added to adjust the pH to 10.4 (as measured in a 1/100 diluted portion of the gel) to avoid impurities such as ETS-4 or quartz in the ETS-10 membrane. Hydrothermal synthesis was carried out at 230 °C for different times (8–48 h) in teflon-lined autoclaves with a volume of 160 mL. Membranes have been labelled ETS10-*x*, where *x* indicates the synthesis time.

Separation experiments were carried out by placing the membrane in a stainless steel cylindrical membrane module where it was sealed with silicone o-rings. A 100 mL(STP)/min mass-flow controlled stream of equimolar mixture (CO_2/N_2 or CO_2/H_2) was fed to the ETS-10 membrane. The permeate side (the inside of the tube) could be flushed with Ar sweep gas to create the necessary driving force. A back pressure regulator at the retentate side was used to control the pressure difference across the membrane (ΔP), while keeping the pressure in the permeate side at atmospheric pressure. The exit stream from the permeate side was analyzed by on-line micro-GC. The CO_2/N_2 or CO_2/H_2 separation factor (α_{CO_2/N_2} or α_{CO_2/H_2}) was calculated as follows:

$$\alpha_{CO_2/N_2,H_2} = \frac{y_{CO_2} \cdot x_{N_2,H_2}}{x_{CO_2} \cdot y_{N_2,H_2}}$$

where *x* and *y* are, respectively, the molar fractions in the feed stream and the permeate exit stream.

Membranes were characterized by a novel defect detection technique recently introduced [32]. Local He permeation values were obtained by supplying small amounts of this gas to a limited area of the membrane surface using a microscopic needle. A mass spectrometer (MS) was used as He detector enabling close to real time analysis. The permeate side of the membrane was swept with N_2 to flush out permeated He from the module. The sampling tube for the MS was located at the permeate side just under the supplying needle at the feed side, and sample gas was injected to the MS by vacuum. The amount of He detected at various positions

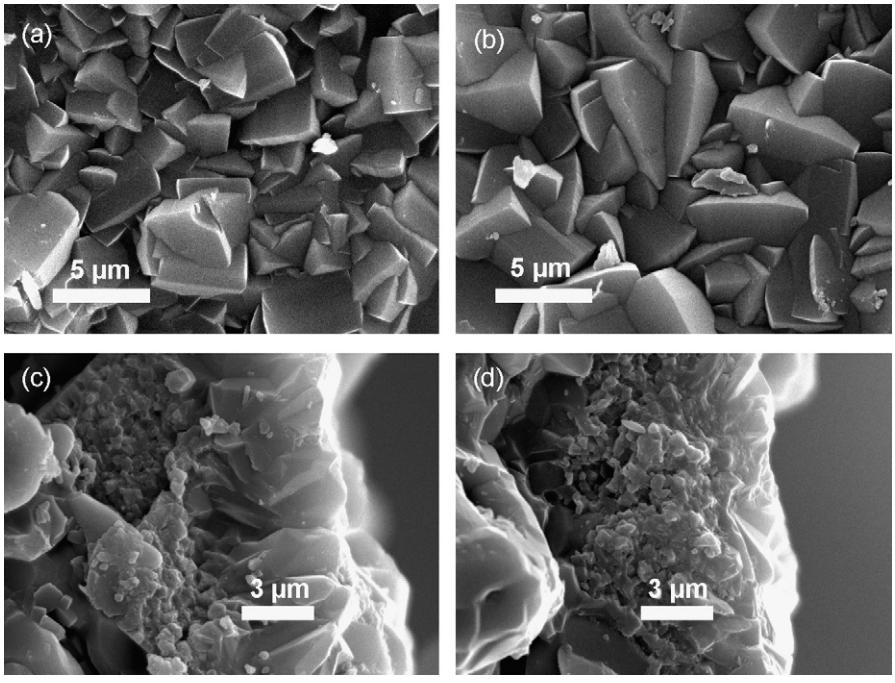

Fig. 1. SEM images of membranes prepared with different synthesis times. Top view (a) and cross-section (c) of membrane ETS10-8. Top view (b) and cross-section (d) of membrane ETS10-24.

gives information about the local He permeation. If we assume similar inherent membrane permeability going from one local area to the next, an abrupt change in the permeation thus indicates a higher local concentration of defects. By changing the position of the needle, a distribution in defect concentration over the membrane surface can be obtained. At the test station, both the needle and sampling tube were fixed while the membrane was moved. The membrane position, in terms of both length and rotating angle, was precisely controlled by a moving stage that has accuracy of few micrometers. The samples were also examined by scanning electron microscopy (SEM) in a JEOL JSM-6400 instrument operating at 3–20 kV.

3. Results and discussion

3.1. Membrane characterization

Table 1 shows the weight gain of the membrane during synthesis (mg of zeolite/g of support), and the corresponding permeances and separation properties. As the weight gain increases with synthesis time, the N_2 single gas permeance, CO_2 permeance in the CO_2/N_2 mixture and the C_3H_6 permeance in the C_3H_6/C_3H_8 mixture decrease. These trends of permeances can be related to the weight gain augmentation (higher resistance to gas transport).

The top section views of membranes ETS10-8 and ETS10-24 (Fig. 1a, b) show an uniform crystal morphology with a truncated bi-pyramid growth typical of ETS-10 material, which size increases with synthesis time from 3–5 μm (8 h) to 6–7 μm (24 h). The cross-section views (Fig. 2c, d) show well intergrown layers of approximately 4–6 μm thicknesses. XRD analysis (not shown, see Ref. [31]) demonstrated that ETS-10 was the main crystalline phase, but contained small quartz impurities after 24 h that noticeably increased after 48 h of hydrothermal treatment.

Fig. 2 shows the signal from the He permeation mapping carried out over ETS10-8, ETS10-24 and ETS10-48 membrane surfaces after converting to colour contrast. Red colour (light grey in printed version) means high He permeation (6–9 times higher than average), blue or black means background intensity. The left and right ends of the figure correspond to the membrane edge, and *x*-axis is the direction along the membrane length, while *y*-axis corresponds to the distance along the circumference. From this it can be seen in Fig. 2 that the ETS10-8 membrane has an important quantity of defects (red colour), whereas ETS10-48 has defects but in lower amount. Finally, ETS10-24 membrane appears "defect-free", i.e. He permeation is too low to be detected. These results suggest that when synthesis time increases defects are removed through intergrowth but with longer synthesis time defects appear again probably due to some dissolution-crystallization processes as already observed for long-term synthesis of other microporous titanosilicate materials [33]. This is in agreement with previous work related to these membranes [31] where synthesis for 48 h gave lower reproducibility and selectivity (see Table 1) in the separation of propylene from a 30/70 C_3H_6/C_3H_8 mixture than membranes with shorter synthesis time. In conclusion, membranes that are synthesized for a too long period seem to have an important amount of permeation defects and did not show important separation selectivity.

3.2. Separation properties

Table 1 and Figs. 3 and 4 show that ETS10-24 membrane can separate CO_2 from N_2 in a binary mixture of CO_2/N_2. This is probably because CO_2 has a stronger electrostatic quadrupole than N_2 that translates into a preferential adsorption of CO_2. It has been previously suggested in the literature that ETS-10 is a basic material and can adsorb CO_2 at low temperature [34]. Thus, it can be expected

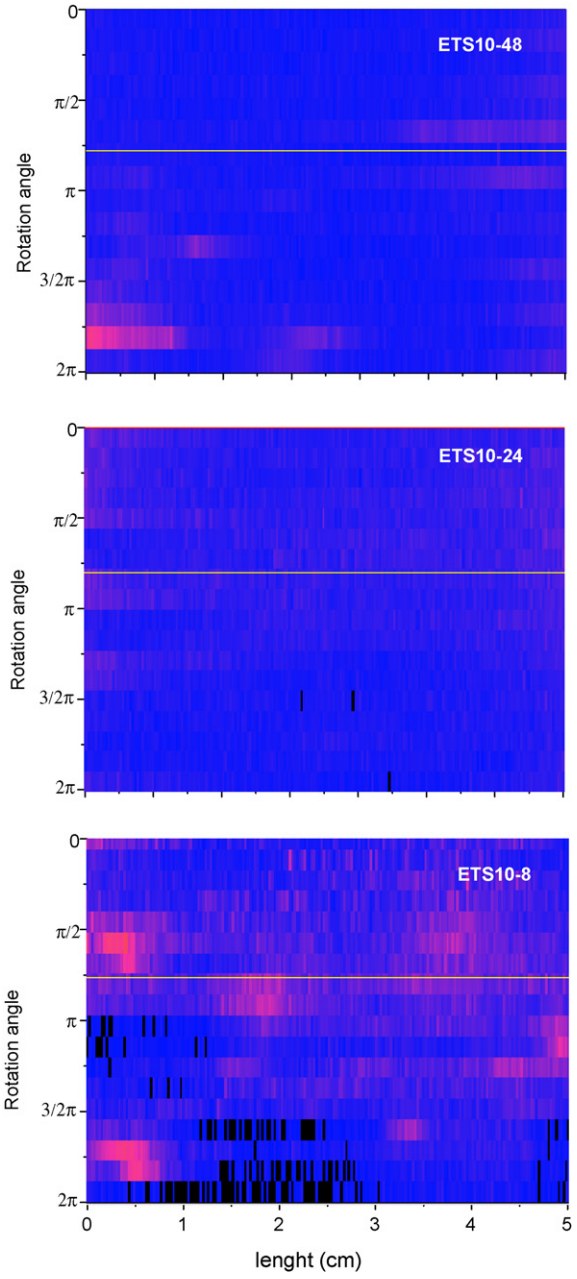

Fig. 2. From top to bottom, leak mapping of ETS10-48, ETS10-24 and ETS10-8 membranes. Red colour indicates high He permeation. Line scan rate was 0.2 cm/min. The membrane was rotated 20° after each line scan. (For interpretation of the references to colour in this figure legend, the reader is referred to the web version of the article.)

that surface diffusion of CO_2 could make a significant contribution to its permeation. Furthermore, adsorbed CO_2 is expected to reduce the N_2 permeation by hindrance resulting in overall CO_2 selectivity in CO_2/N_2 mixtures [11,14–16].

In Fig. 3, CO_2 and N_2 fluxes increase with increase pressure differential. At low pressure, the CO_2 flux increases more than the N_2 flux due to the higher adsorption capacity of ETS-10 for the CO_2 molecule. At higher pressure the flux seems to approach asymptotically to a line of constant slope with N_2 flux having the steeper slope. In this pressure region, the ETS-10 surface is probably saturated with CO_2. As a consequence, the hindrance efficiency of CO_2 to N_2 transport is reaching a maximum and further increase in pressure differential favours Knudsen diffusion through defects. Knudsen diffusion is governed by the pressure difference across the membrane, and lighter molecules are faster, thus N_2 diffusion is favoured.

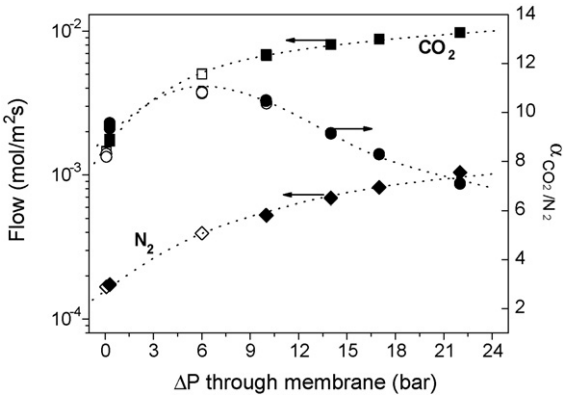

Fig. 3. N_2 (♦) and CO_2 (■) permeation fluxes and separation factor (●) for a CO_2/N_2 mixture (50% molar each) as a function of pressure difference across membrane ETS10-24. Room temperature and permeate at atmospheric pressure. Ar sweep gas flow rate: 60 mL(STP)/min. Hollow symbols correspond to the flow value after high-pressure testing.

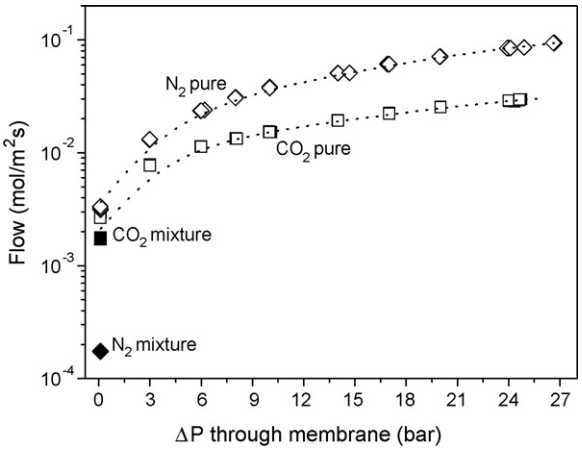

Fig. 5. N_2 (◊) and CO_2 (□) single permeation fluxes at variable pressure in the retentate of membrane ETS10-24. N_2 and CO_2 permeation in equimolar mixture (♦ and ■, respectively) with $\Delta P = 0.29$ bar from Fig. 3. Room temperature and Ar sweep gas flow rate: 60 mL(STP)/min.

According to the above described behavior, a broad maximum of 10.8 appears in the CO_2/N_2 separation factor at pressure about 6 bar (Fig. 3). It should be noted that in spite of the decrease in selectivity, its value is still 7.0 at 22 bar. As an additional check, experiments at lower pressures (hollow points in Fig. 3) were repeated after the highest pressure points in Fig. 3. Similar values were found, assuring the stability and mechanical resistance to high pressure of the membrane.

The influence of sweep gas in CO_2/N_2 separation with ETS10-24 membrane can be observed in Fig. 4. CO_2 flux increases slightly and less than N_2 flux. In principle, the sweep gas increases the driving force for permeation by lowering the CO_2 and N_2 concentration at the permeate side. In addition, higher sweep gas flow rates are expected to increase the mass transfer coefficient at the permeate side, accelerating desorption of the permeated species and decreasing the CO_2 concentration to values beyond those necessary to maintain an efficient pore blockage, and consequently the separation factor decreases.

Fig. 5 shows the variation of N_2 and CO_2 fluxes in pure gas experiments with the ETS10-24 membrane compared to those of N_2 and CO_2 in the corresponding mixture (closed points) at low pressure. Single N_2 and CO_2 permeation fluxes are quite similar probably due to the similarity of molecular size between CO_2 and N_2 (0.33 and 0.37 nm for CO_2 and N_2, respectively). The shape of both permeation curves agrees with an adsorption–diffusion mechanism determined by a Langmuir isotherm. In the pressure range studied, CO_2 has almost arrived at saturation values, while N_2 permeation increases yet slightly indicating a weak adsorption of N_2. It may be seen that in the mixture the CO_2 flux was not significantly affected by the presence of N_2. On the contrary, the N_2 flux abruptly decreases (when compared to that of pure component) demonstrating that preferential strong adsorption of CO_2 blocks or reduces the membrane pores diminishing N_2 flux.

Membrane ETS10-24 was also tested in the CO_2/H_2 separation (see Table 1). At ΔP close to 0, a CO_2/H_2 separation factor of 9.0 was obtained with an equimolecular mixture corroborating that CO_2 sorption hinders H_2 flux through the ETS-10 membrane. CO_2 permeance in this mixture is 1.9×10^{-8} mol/m^2 s Pa in agreement with the value found in the mixture CO_2/N_2 (see Table 1).

CO_2/N_2 separation was also performed with membrane ETS10-8 (Fig. 6), i.e. the membrane synthesized in only 8 h. Separation factor is 6 with ΔP close to 0 but when pressure increases separation factor decreases to values below 1. This small value for the separation factor means that CO_2 and N_2 transport takes place through defects that could be controlled by Knudsen flow. These results are in accordance with the leak mapping (Fig. 2) where ETS10-8 membrane has shown as significant quantity of defects. After the high pressure measurements, the lowest pressure measurement was repeated giving again a high separation factor. This confirmed again the mechanical stability of the membrane.

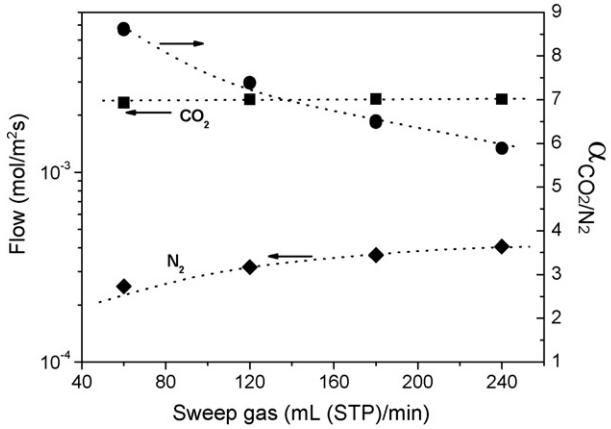

Fig. 4. N_2 (♦) and CO_2 (■) permeation fluxes and separation factors (●) for a CO_2/N_2 mixture (50% molar each), at variable Ar sweep gas flow rate of membrane ETS10-24. Room temperature, permeate at atmospheric pressure and $\Delta P = 0.08$ bar.

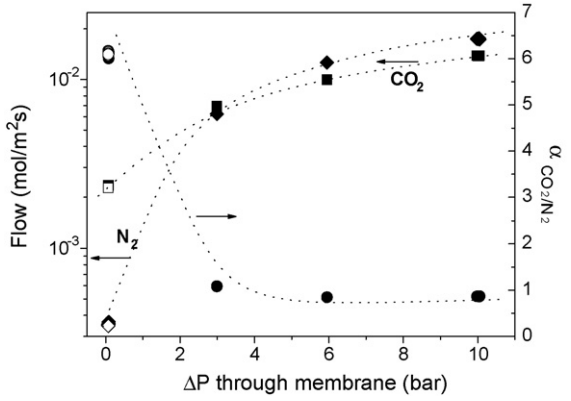

Fig. 6. N_2 (♦) and CO_2 (■) permeation fluxes and separation factors (●) for a CO_2/N_2 mixture (50% molar each), at variable pressure in the retentate of membrane ETS10-8. Room temperature, Ar sweep gas flow rate: 60 mL(STP)/min and $\Delta P = 0.08$ bar. Hollow symbols correspond to the flow value after high-pressure tests.

4. Conclusions

In this work, the following conclusions can be drawn:

1. ETS-10 membranes without visible defects as mapped by local He permeation can separate CO_2 from binary mixtures of CO_2/N_2 and CO_2/H_2 by preferential adsorption and diffusion of CO_2. For CO_2/N_2 mixtures, maximum separation factors between 7 and 10 were obtained in the 6–22 bar pressure range.
2. There is an optimum synthesis time for ETS-10 membranes. When synthesis time becomes too long, new defects are formed. Under the experimental conditions of this work, 24 h of hydrothermal treatment is the optimum synthesis time to obtain selective membranes.
3. Leak mapping is a characterization technique to visualize defects in microporous zeolite membranes by simple, non-destructive analysis. There exists a clear correlation between the leak mapping results and the selectivity of the investigated membranes.

Acknowledgements

Financial support from MEC (MAT2007-61028) in Spain and ENGAS (The 6th Framework Programme of the European Commission, RITA-CT-2003-506502) is gratefully acknowledged.

References

[1] A. Damle, T. Dorchak, Recovery of carbon dioxide in advanced fossil energy conversion processes using a membrane reactor, J. Energy Environ. Res. 1 (2001) 77–89.
[2] H. Lin, B. Freeman, Gas solubility, diffusivity and permeability in poly(ethylene oxide), J. Membr. Sci. 239 (2004) 105–117.
[3] C. Powell, G. Qiao, Polymeric CO_2/N_2 gas separation membranes for the capture of carbon dioxide from power plant flue gases, J. Membr. Sci. 279 (2006) 1–49.
[4] H. Zhao, Y. Cao, X. Ding, M. Zhou, Q. Yuan, Poly(N,N-dimethylaminoethyl methacrylate)–poly(ethylene oxide) copolymer membranes for selective separation of CO_2, J. Membr. Sci. 310 (2008) 365–373.
[5] K. Kusakabe, T. Kuroda, S. Mooroka, Separation of carbon-dioxide from nitrogen using ion-exchanged faujasite-type zeolite membranes formed on porous support tubes, J. Membr. Sci. 148 (1998) 13–23.
[6] T. Tomita, K. Nakayama, H. Sakai, Gas separation characteristics of DDR type zeolite membrane, Micropor. Mesopor. Mater. 68 (2004) 71–75.
[7] A. Yamasaki, An overview of CO_2 mitigation options for global warming—emphasizing CO_2 sequestration options, J. Chem. Eng. Jpn. 36 (2003) 361–375.
[8] S. Nair, Z. Lai, V. Nikolakis, G. Xomeritakis, G. Bonilla, M. Tsapatsis, Separation of close-boiling hydrocarbon mixtures by MFI and FAU membranes made by secondary growth, Micropor. Mesopor. Mater. 48 (2001) 219–228.
[9] J. Coronas, J. Santamaría, Separations using zeolite membranes, Sep. Purif. Methods 28 (1999) 127–177.
[10] T. Bowen, R. Noble, J. Falconer, Fundamentals and applications of pervaporation through zeolite membranes, J. Membr. Sci. 245 (2004) 1–33.
[11] K. Kusakabe, T. Kuroda, A. Murata, S. Morooka, Formation of a Y-type zeolite membrane on a porous α-alumina, Ind. Eng. Chem. Res. 36 (1997) 649–655.
[12] K. Kusakabe, T. Kuroda, K. Uchino, Y. Hasegawa, S. Mooroka, Gas permeation properties of ion-exchanged Faujasite-type zeolite membranes, AIChE J. 14 (1999) 1220–1226.
[13] Y. Hasegawa, K. Watanabe, K. Kusakabe, S. Morooka, The separation of CO_2 using Y-type zeolite membranes ion-exchanged with alkali metal cations, Sep. Purif. Technol. 22–23 (2001) 319–325.
[14] M.C. Lovallo, A. Gouzinis, M. Tsapatsis, Synthesis and characterization of oriented membranes prepared by secondary growth, AIChE J. 44 (1998) 1903–1913.
[15] L. van den Broeke, F. Kapteijn, J. Moulijn, Transport and separation properties of a silicalite-1 membrane-II. Variable separation factor, Chem. Eng. Sci. 54 (1999) 259–269.
[16] M.P. Bernal, J. Coronas, M. Menéndez, J. Santamaria, Separation of CO_2/N_2 mixtures using MFI-Type zeolite membranes, AIChE J. 50 (2004) 127–135.
[17] V. Sebastián, I. Kumakiri, R. Bredesen, M. Menéndez, Zeolite membrane for CO_2 removal: operating at high pressure, J. Membr. Sci. 292 (2007) 92–97.
[18] D.W. Shin, S.H. Hyun, C.H. Cho, M.H. Han, Synthesis and CO_2/N_2 gas permeation characteristics of ZSM-5 zeolite membranes, Micropor. Mesopor. Mater. 85 (2005) 313–323.
[19] J. Poshusta, V. Tuan, E. Pape, R. Noble, J. Falconer, Separation of light gas mixtures using SAPO-34 membranes, AIChE J. 46 (2000) 779–789.
[20] S. Li, J. Falconer, R. Noble, SAPO-34 membranes for CO_2/CH_4 separation, J. Membr. Sci. 241 (2004) 121–135.
[21] S. Li, J. Falconer, R. Noble, SAPO-34 membranes for CO_2/CH_4 separations: effect of Si/Al ratio, Micropor. Mesopor. Mater. 110 (2008) 310–317.
[22] S. Kuznicki, Large-pored crystalline titanium molecular sieve zeolites, United States Patent 4 853 202 (1989).
[23] S. Kuznicki, Preparation of small-pored crystalline titanium molecular sieve zeolites, United States Patent 4 938 939 (1990).
[24] E. Doskocil, Ion-exchanged ETS-10 catalysts for the cycloaddition of carbon dioxide to propylene oxide, Micropor. Mesopor. Mater. 76 (2004) 177–183.
[25] Y. Krisnandi, R. Howe, Effects of ion-exchange on the photoreactivity of ETS-10, Appl. Catal. A: Gen. 307 (2006) 62–69.
[26] I. Tiscornia, S. Irusta, P. Prádanos, C. Téllez, J. Coronas, J. Santamaría, Preparation and characterization of titanosilicate Ag-ETS-10 for propylene and propane adsorption, J. Phys. Chem. C 111 (2007) 4702–4709.
[27] S. Kuznicki, V. Bell, S. Nair, H. Hillhouse, R. Jacubinas, C. Braunbarth, B. Toby, M. Tsapatsis, A titanosilicate molecular sieve with adjustable pores for size-selective adsorption of molecules, Nature 412 (2001) 720–724.
[28] Z. Lin, J. Rocha, A. Navajas, C. Téllez, J. Coronas, J. Santamaría, Synthesis and characterisation of titanosilicate ETS-10 membranes, Micropor. Mesopor. Mater. 67 (2004) 79–86.
[29] H. Kita, X. Li, K. Takei, X. Zhang, K. Okamoto, K. Itabashi, Synthesis of highly acid-resistant zeolite membranes and their permeation properties, in: F. Akin, Y. Lin (Eds.), Proceedings of the 8th International Conference on Inorganic Membranes, Cincinnati, USA, 2004, pp. 250–253.
[30] I. Tiscornia, Z. Lin, J. Rocha, C. Téllez, J. Coronas, J. Santamaría, Preparation of titanosilicate ETS-10 and vanadosilicate AM-6 membranes, Stud. Surf. Sci. Catal. 158 (2005) 423–430.
[31] I. Tiscornia, S. Irusta, C. Téllez, J. Coronas, J. Santamaría, Separation of propylene/propane mixtures by titanosilicate ETS-10 membranes prepared in one-step seeded hydrothermal synthesis, J. Membr. Sci. 311 (2008) 326–335.
[32] I. Kumakiri, M. Stange, T. Peters, H. Klette, H. Kita, R. Bredesen, Membrane characterisation by a novel defect detection technique, Micropor. Mesopor. Mater. 115 (2008) 33–39.
[33] V. Sebastián, C. Téllez, J. Coronas, J. Santamaría, Formation of micro/macroporous hierarchical spheres of titanosilicate umbite, Eur. J. Inorg. Chem. (2008) 2448–2453.
[34] F.X. Llabrés i Xamena, A. Zecchina, FTIR spectroscopy of carbon dioxide adsorbed on sodium- and magnesium-exchanged ETS-10 molecular sieves, Phys. Chem. Chem. Phys. 4 (2002) 1978–1982.